Title

Global Transcriptional Response to CRISPR/Cas9-AAV6-Based Genome Editing in CD34+ Hematopoietic Stem and Progenitor Cells.

Journal

Molecular Therapy, 26(10)

Authors

Cromer, M
Vaidyanathan, Sriram
Ryan, Daniel
et al.

Publication Date

2018-10-03

DOI

10.1016/j.ymthe.2018.06.002

Peer reviewed

Molecular Therapy
Original Article

Global Transcriptional Response to CRISPR/Cas9-AAV6-Based Genome Editing in CD34$^+$ Hematopoietic Stem and Progenitor Cells

M. Kyle Cromer,[1] Sriram Vaidyanathan,[1] Daniel E. Ryan,[2] Bo Curry,[2] Anne Bergstrom Lucas,[2] Joab Camarena,[1] Milan Kaushik,[1] Sarah R. Hay,[1] Renata M. Martin,[1] Israel Steinfeld,[2] Rasmus O. Bak,[1] Daniel P. Dever,[1] Ayal Hendel,[3] Laurakay Bruhn,[2] and Matthew H. Porteus[1]

[1]Department of Pediatrics, Stanford University, Stanford, CA 94305, USA; [2]Agilent Technologies, Santa Clara, CA 95051, USA; [3]Institute for Nanotechnology and Advanced Materials, The Mina and Everard Goodman Faculty of Life Sciences, Bar-Ilan University, Ramat Gan 5290002, Israel

Genome-editing technologies are currently being translated to the clinic. However, cellular effects of the editing machinery have yet to be fully elucidated. Here, we performed global microarray-based gene expression measurements on human CD34$^+$ hematopoietic stem and progenitor cells that underwent editing. We probed effects of the entire editing process as well as each component individually, including electroporation, Cas9 (mRNA or protein) with chemically modified sgRNA, and AAV6 transduction. We identified differentially expressed genes relative to control treatments, which displayed enrichment for particular biological processes. All editing machinery components elicited immune, stress, and apoptotic responses. Cas9 mRNA invoked the greatest amount of transcriptional change, eliciting a distinct viral response and global transcriptional downregulation, particularly of metabolic and cell cycle processes. Electroporation also induced significant transcriptional change, with notable downregulation of metabolic processes. Surprisingly, AAV6 evoked no detectable viral response. We also found Cas9/sgRNA ribonucleoprotein treatment to be well tolerated, in spite of eliciting a DNA damage signature. Overall, this data establishes a benchmark for cellular tolerance of CRISPR/Cas9-AAV6-based genome editing, ensuring that the clinical protocol is as safe and efficient as possible.

INTRODUCTION

Due to improvements in the specificity and efficiency of genome editing, this technology is now being translated to the clinic. These advancements have occurred across a number of genome-editing systems, including those that employ zinc-finger nucleases (ZFNs), TAL-effector nucleases (TALENs), megaTALs, and CRISPR/Cas9. All of these systems are able to initiate a double-strand break (DSB) in the DNA at a specific location in the genome. Following creation of a DSB, the cell uses one of two pathways for repair, non-homologous end joining (NHEJ), or homology-directed repair (HDR).[1] NHEJ is an error-prone pathway most useful for introducing loss-of-function mutations. However, editing for gene-correction purposes exploits the HDR pathway in order to introduce specific changes to the genome with single-nucleotide resolution. This can be done by delivering a gene-targeting donor template for DNA damage repair, incorporating the custom edit(s) with homology arms spanning the cut site. In doing so, the HDR pathway uses these single- or double-stranded donor templates to introduce custom, scarless edits into the genome by processes known as single-stranded template repair (SSTR) or homologous recombination (HR), respectively.

Here, we employ the CRISPR/Cas9 system, where targeting specificity is imparted to the Cas9 protein when it forms a complex with a single-guide RNA (sgRNA) sequence.[2–5] It is possible to deliver Cas9:sgRNA using lipofection, although this method has been shown to cause significant cytotoxicity compared to electroporation, which is a process used to increase membrane permeability by applying an electrical field to cells.[6] Not only are there multiple methods for delivering Cas9:sgRNA, but the form in which it is delivered may also vary. It may be introduced transiently as Cas9 protein pre-complexed with sgRNA (known as ribonucleoprotein [RNP]), as Cas9 mRNA separately with sgRNA,[7] or from a DNA expression plasmid. Comparatively, Cas9 and sgRNA in the form of a DNA plasmid has been shown to exhibit the greatest cellular toxicity.[7] On the other hand, electroporation of Cas9:sgRNA in the form of RNP has been shown to not only elicit the least cytotoxicity, but the greatest enzymatic activity as well.[8]

There also exists a variety of methods for donor template delivery, such as integrase-deficient lentiviral systems,[9] single-stranded oligodeoxynucleotides (ssODNs),[10] and adeno-associated viruses (AAVs).[11,12]

Received 6 December 2017; accepted 1 June 2018;
https://doi.org/10.1016/j.ymthe.2018.06.002.

Correspondence: Matthew H. Porteus, Department of Pediatrics, Stanford University, Stanford, CA 94305, USA.
E-mail: mporteus@stanford.edu
Correspondence: Ayal Hendel, Institute for Nanotechnology and Advanced Materials, The Mina and Everard Goodman Faculty of Life Sciences, Bar-Ilan University, Ramat Gan 5290002, Israel.
E-mail: ayal.hendel@biu.ac.il

Due to safety considerations and technical limitations of alternative systems, we chose to use AAV, a classic gene-targeting vector that utilizes HR to introduce single-nucleotide edits or large insertions, that has proven to be an effective and clinically compatible delivery vehicle in a wide variety of cell types, particularly in $CD34^+$ hematopoietic stem and progenitor cells (HSPCs).[8,11,13–16]

Genome editing that combines these two technologies, Cas9-mediated DSB formation with AAV donor template delivery, has been successfully employed for translational as well as basic science purposes.[8] However, the editing process itself has been reported to cause cytotoxicity *in vitro*[17] as well as an immunological reaction when applied by *in vivo* electroporation in mice.[18] This is thought to be due, in part, to DNA damage caused by Cas9-induced DSBs, particularly when off-target cutting occurs at multiple locations throughout the genome.[19] It is unclear whether the same cytotoxicity is seen when sgRNAs with low levels of off-target activity are employed. Further efforts to reduce cytotoxicity have also explored the effect of incorporating chemical modifications on both the Cas9 mRNA[20] as well as the sgRNA,[7,21,22] which has proven to be an effective means to reduce immune detection, improve stability, and reduce cytotoxicity during this process. In addition, electroporation,[23] delivery of exogenous mRNA,[8] and AAV transduction[24] have been shown to also elicit cytotoxicity in a variety of cell lines and primary patient-derived cells. It is currently unclear which elements of the protocol are most responsible for this toxicity, much less which specific genes and pathways may be involved in this response. Identifying these specific genes and pathways could enable us to further optimize genome-editing protocols.

To understand the immediate transcriptional response evoked by the entire editing procedure, total RNA isolated from human primary $CD34^+$ cells that underwent genome editing was applied to DNA microarrays in order to measure global gene expression. The cells were also treated with separate components of the editing machinery—electroporation, Cas9 (as mRNA or protein) complexed with sgRNA and AAV—to parse out the individual contribution of each to the transcriptional response. Toward this end, we chose to employ this experimental design in a clinically relevant genome-editing model that has been used to successfully edit the β-globin (*HBB*) gene, which harbors the missense mutation responsible for sickle cell disease (SCD), in HSPCs.[8] Therefore, all of our transcriptional analysis was performed on $CD34^+$ HSPCs that were treated with all or some of the editing machinery used to edit a single-nucleotide polymorphism (SNP) within the *HBB* gene.

Through these experiments, we identified that (1) Cas9 mRNA invokes a strong anti-viral response that results in global transcriptional repression; (2) AAV6 transduction elicits no detectable viral response in $CD34^+$ HSPCs; (3) Cas9 RNP induces a DNA damage response even in the case of sgRNAs with low off-target activity.

These results yield important insights into the global transcriptional response to genome-editing machinery in human cells. These results may also prove useful in further refinement of the genome-editing protocol in clinically relevant cell types.

RESULTS

Experimental Design to Probe the Transcriptional Response to Genome-Editing Machinery

We chose to probe the global transcriptional response to the genome-editing process using the established and clinically relevant model of SCD. SCD is caused by one SNP (A to T), which results in a glutamic acid to valine missense mutation at codon 6 (Glu6Val) of the *HBB* gene.[25,26] Because of the difficulty in obtaining HSPCs from SCD patients, we instead demonstrated our ability to edit this locus by introducing the SCD-causing SNP into HSPCs isolated from wild-type (WT) patients.[8] Therefore, in this study we treated $CD34^+$ WT HSPCs with all or some of the components of the editing machinery used to introduce the Glu6Val SCD-causing mutation.

Because donor variation is well-documented for aspects of the editing process,[27] we performed these treatments on HSPCs isolated from four individual donors. This allowed our downstream analysis to parse out effects of the editing machinery that are common across multiple donors. Using multiple $CD34^+$ HSPC donors also allowed us to gauge which has a greater bearing on global transcription—the editing machinery or the donor of origin.

The kinetics of Cas9-induced DSB initiation has only recently been reported and depicts a highly time-dependent process.[28] Therefore, in order to be confident that we were capturing the immediate transcriptional response to genome editing, we chose to measure global transcription post-treatment at early (6 hr) and late (24 hr) time points.

Accordingly, we performed the following treatment groups across four donors and two time points with two technical replicates per sample: mock electroporation (hereafter hereafter abbreviated as "elec"), electroporation of Cas9 mRNA and sgRNA ("mRNA"), electroporation of Cas9 mRNA and sgRNA followed by AAV6 transduction ("mRNA + AAV"), electroporation of Cas9 protein complexed with sgRNA ("RNP"), and electroporation of Cas9 protein and sgRNA followed by AAV6 transduction ("RNP + AAV"). We also performed the following treatment groups only at the 24 hr time point: no electroporation negative control ("not elect.") and AAV6 transduction alone ("AAV"). When employed, electroporation was performed using a Lonza Nucleofector 2b. Due to improved tolerance and activity, sgRNAs with 2′-O-methyl-3′-phosphorothioate modification at the three terminal positions at both 5′ and 3′ ends were used where applicable.[7] The Cas9 mRNA that was used in this study was produced commercially with 5-methylcytidine and pseudouridine modifications, which have been shown to reduce innate antiviral responses.[20] For this study, *S. pyogenes* Cas9 protein was commercially produced and purified. AAV6 was produced in HEK293 cells and purified using the iodixanol density gradient ultracentrifugation method as previously reported.[29] AAV6 was titered using qPCR with probes corresponding to the inverse

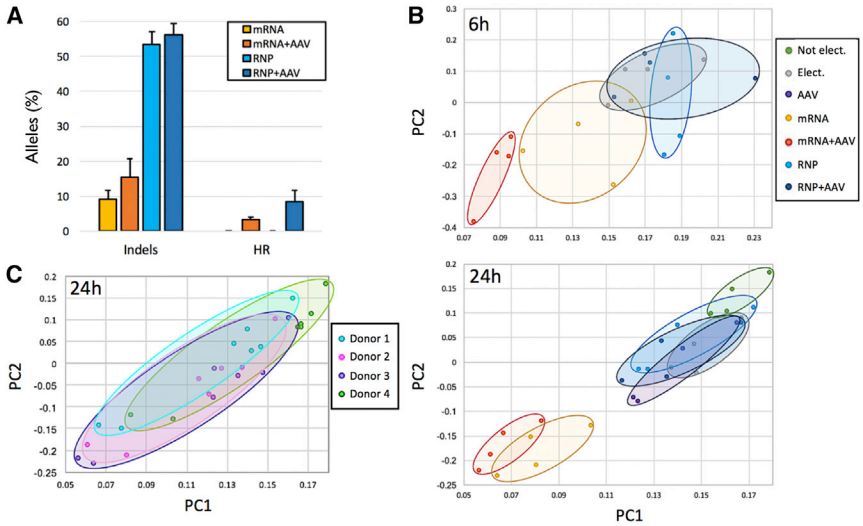

Figure 1. Unsupervised Clustering Reveals Cas9 mRNA-Induced Expression Signature

(A) Indel rates and HR rates per treatment group are plotted as determined by TIDER analysis and TOPO cloning, respectively. Each column represents four HSPC $CD34^+$ donors. All columns are means and error bars depict SEM. (B) At 6 hr and 24 hr post-treatment, two principal components (PC1 and PC2) accounting for majority of variation are plotted for each treatment for each donor, grouped by treatment. (C) At 24 hr post-treatment, two principal components (PC1 and PC2) accounting for majority of variation are plotted for each treatment for each donor, grouped by donor. Signals from all probes on the microarray were used as input for unsupervised clustering by PCA. Each data point represents the average PC1 and PC2 values of two technical replicates for an individual $CD34^+$ donor for each treatment.

terminal repeat region[30] and applied to cells at a MOI of 5E4 vector genomes per cell.

For treatment groups expected to have significant formation of insertions and deletions (indels; resulting from erroneous NHEJ repair of DSBs) and HR (resulting from recombination of DSBs with AAV6 donor template), we measured each using TIDER software[31,32] and analysis of Sanger sequencing reads from individual TOPO-cloned PCR fragments, respectively (Figure 1A). As previously reported, we observed greater rates of indel formation when Cas9 was delivered in the form of protein complexed with sgRNA (RNP) than Cas9 in the form of mRNA.[8] This likely also accounts for the greater frequencies of HR that were observed when delivering Cas9 in the form of RNP. As expected, HR was only detected when Cas9 was delivered along with a DNA repair template via AAV.

Unsupervised Clustering Identifies Treatment-Specific Effects on the Transcriptome

Once microarray measurements were performed on all samples, we determined whether treatment or donor-of-origin more heavily influenced gene-expression profiles. Toward this end, we performed unsupervised clustering of the microarray signals via principal component analysis (PCA) on all samples at both 6-hr and 24-hr time points (Figure S1A). Following this unbiased clustering, samples were grouped by treatment group (Figures 1B and S1B) as well as by mobilized peripheral blood donor (Figure 1C). In doing so, we observed that samples formed more distinct clusters when grouped by treatment rather than by donor, indicating that exposure to specific components of the editing machinery more heavily affects global transcription than the expression patterns inherent to each individual donor. When grouped by treatment, the mRNA and mRNA + AAV samples appeared to form a distinct separate cluster relative to all other samples. This was further confirmed by unsupervised hierarchical clustering, which indicated that the greatest single difference between all treatments was whether or not they were electroporated with Cas9 mRNA (Figure S2).

In order to complement this analysis, we sought to quantify Euclidean distance as a measure of similarity. We did so by deriving a cluster score for all samples, including technical replicates, which represented degree of variation across principal components (average of individual standard deviations across each of the top three principal components for a specific grouping) (Figures S3 and S4). A lower cluster score indicates greater similarity within a particular grouping. This allowed us to more conclusively determine not only that technical replicates more closely resembled each other than any other sample, but also that treatment had a greater bearing on transcription than the patient that the cells were derived from.

Transcriptional Response to Editing Is Greatest at 24 hr

In order to determine the gene-level transcriptional response to editing machinery, we calculated the expression difference between each treatment and appropriate control for all probes measured on the arrays. Because these experiments were performed on samples from four individual donors, we were able to derive p values (expressed as $-\log_{10}$(p value), or "MLogP") for the log2 expression ratio of each probe between treatment and control samples. We then plotted these values in the form of volcano plots for each treatment at each time point (Figures 2 and S5). Accounting for multiple comparisons, the Bonferroni-adjusted significance threshold was determined to be MLogP ≥ 7 (Table S1). This clearly indicated that the transcriptional response to all of the editing machinery components was more pronounced at 24 hr than at 6 hr. The greatest transcriptional response was elicited when cells were treated with Cas9 mRNA, with a total of 10,666 and 12,201 differentially expressed probes at 24 hr in mRNA and mRNA + AAV samples, respectively (Figure S6). The magnitude of this response is likely the cause of the segregation of Cas9 mRNA samples from all other treatments when we performed hierarchical clustering. Interestingly, we observed a skewing toward

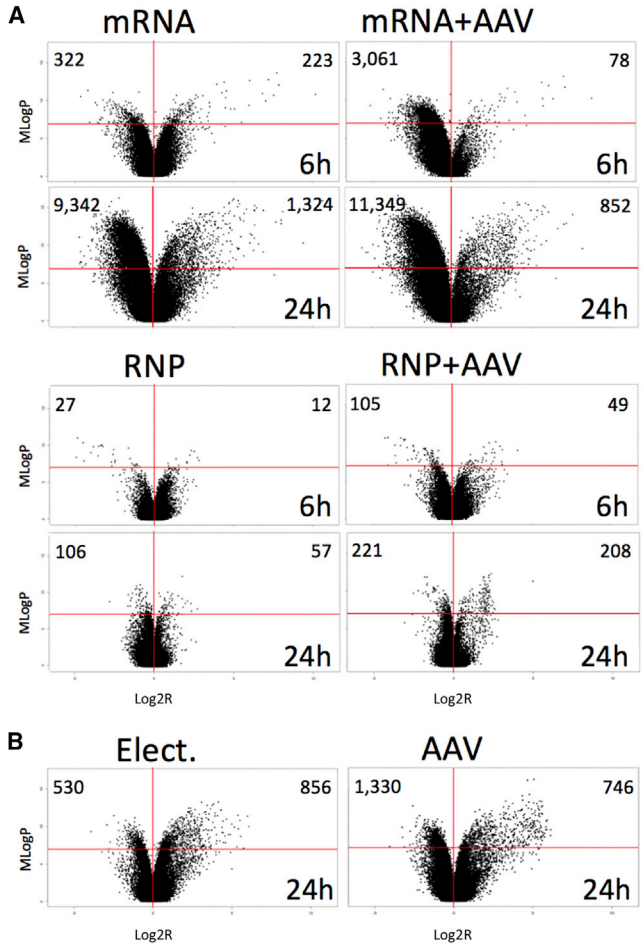

Figure 2. Volcano Plots Depict Differential Expression Signatures of All Treatments

(A) MLogP value is plotted against log2 of the ratio of the probe expression difference between specific treatment and mock electroporation treatment at 6 hr and 24 hr. (B) At 24 hr post-treatment, electroporation and AAV-only samples were compared to non-electroporated control sample. The horizontal line indicates Bonferroni-corrected significance threshold of MLogP $\geq$ 7. The total numbers of significantly down- and upregulated probes is shown in the top left and top right of each plot, respectively.

downregulation compared to the control treatment in Cas9 mRNA-treated samples, suggesting dramatic global transcriptional repression. On the other hand, RNP and RNP + AAV samples appeared to have the least influence on global transcription, with a total of 163 and 429 differentially expressed probes at 24 hr in RNP and RNP + AAV samples, respectively (Figure S6).

Enrichment of Viral, DNA Repair, Mitotic, and Apoptotic GO Processes

We determined whether the sets of differentially expressed probes (corresponding to specific genes) for each treatment were enriched for specific gene ontology (GO) processes. Therefore, we used significantly up- and downregulated genes for each treatment as separate inputs for GO enrichment analysis.[33] Using this approach, we identified significantly enriched up- and downregulated GO processes in all samples at a false discovery rate (FDR) significance threshold of $q \leq 0.01$. We performed this analysis at both 6 hr and 24 hr (Figure S6). As mentioned earlier, we found that not only was the transcriptional response greatest at 24 hr, but the number of enriched GO processes was greatest at this time point as well. Therefore, much of the downstream analysis was performed only on treatments at 24 hr.

As expected, we observed that samples with greater numbers of differentially expressed probes yielded greater numbers of enriched GO processes (Figure S6). Accordingly, the Cas9 mRNA-treated samples possessed the greatest number of enriched GO processes and the Cas9 RNP-treated samples the fewest. Because of their vast number and repetitive nature (Figure S7), we devised a visual representation that grouped enriched GO processes into the most common pathways for all treatments at 24 hr (Figures 3, S8, and S9). We also identified the 10 genes most heavily contributing to the enrichment of these pathways (Figure 4), which appear to depict the same treatment-specific trends.

We found that all components of the editing machinery elicited both immune and stress responses. Though the stress response was similar across all treatments, immune-related processes displayed much greater treatment-specific variation. Cas9 RNP caused a relatively modest immune response in comparison to the dramatic response observed when cells were exposed to either electroporation or Cas9 mRNA. Surprisingly, though AAV6 evoked a moderate immune reaction, we found no significant viral or interferon responses in this treatment group. On the other hand, viral defense and interferon processes were heavily enriched when cells were treated with Cas9 mRNA. In fact, for both mRNA and mRNA + AAV samples, the three most significantly enriched GO processes were "response to virus" (GO, 0009615; FDR q value = 4.0E-31 and 2.1E-28, respectively), "defense response to virus" (GO, 0051607; FDR q value = 5.9E-29 and 1.7E-26, respectively), and "type I interferon signaling pathway" (GO, 0060337; FDR q value = 9.8E-28 and 6.7E-24, respectively) (Table S2).

The samples with the greatest immune response that did not involve viral- or interferon-related processes were those exposed to electroporation, AAV6, and Cas9 mRNA. Interestingly, these were also the samples that possessed the most striking downregulation of metabolic processes (Figures 3 and S9A). Of downregulated processes, the three most significant for both mRNA and mRNA + AAV samples were "cellular metabolic process" (GO, 0044237; FDR q value = 9.4E-73 and 1.9E-101, respectively), "metabolic process" (GO, 0008152; FDR q value = 2.5E-67 and 5.2E-90, respectively), and "organic substance metabolic process" (GO, 0071704; FDR q value = 5.4E-53 and 2.7E-72, respectively) (Table S2). For samples exposed to either electroporation or AAV6, the 10 most significantly downregulated GO processes were metabolic. Though this broad metabolic downregulation occurred in all but Cas9 RNP-treated samples, global transcriptional repression appeared to be unique to Cas9 mRNA treatments

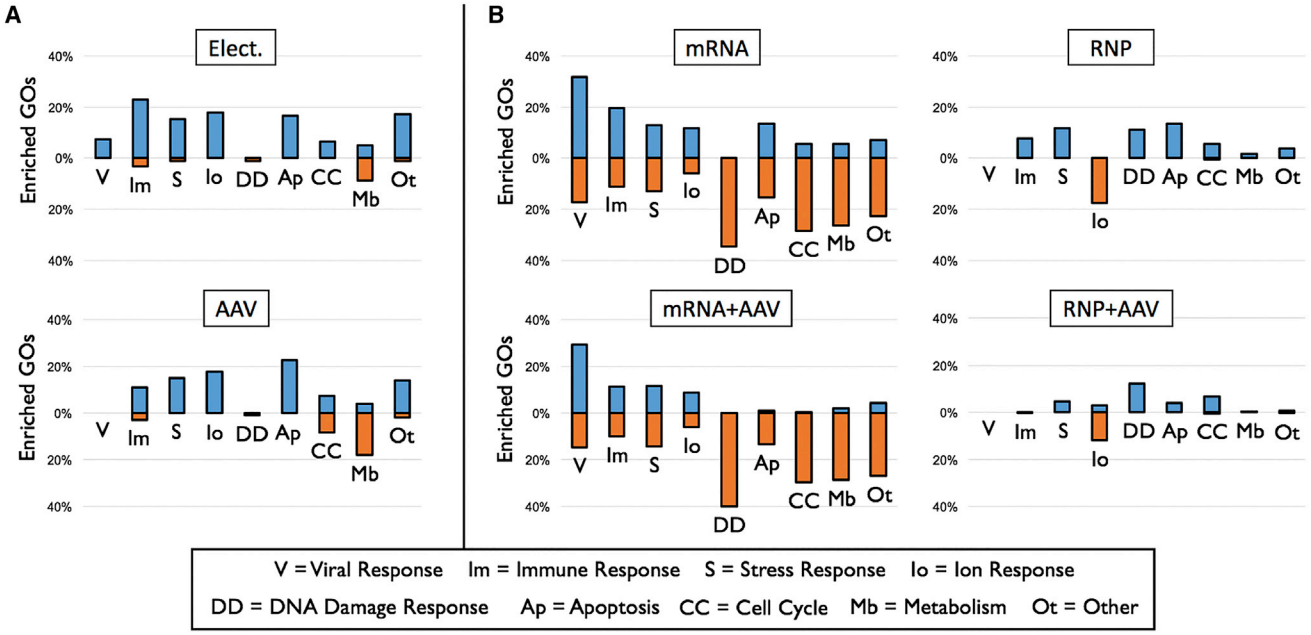

Figure 3. Cas9 mRNA and Electroporation Treatments Elicit Greatest Cellular Response

(A) At 24 hr post-treatment, percentage of enriched GO processes (FDR q value $\leq$ 0.01) normalized by total number in each category across all treatments are plotted for electroporated and AAV treatments compared to non-electroporated control. (B) At 24 hr post-treatment, normalized percentage of enriched GO processes compared to electroporated control. GO processes differentially up- or downregulated are shown in blue and orange, respectively. All differentially expressed genes as well as enriched GO processes are provided in Tables S1 and S2, respectively.

(Figures 3, S8, and S9). Such global transcriptional and translational repression has been reported as a result of the type I interferon response.[34,35]

Our genome-editing protocol used Cas9 to successfully initiate DSB breaks, as indicated by significant indel formation (Figure 1A). As a consequence, it is not surprising that we observed a DNA damage response (DDR) signature that was most apparent in Cas9 RNP samples. Within differentially upregulated genes, Cas9 RNP-treated samples at 24 hr possessed the greatest number of DDR-related GO processes (Figures 3 and S8). We did not observe enrichment of DDR pathways at the earlier 6-hr time point (data not shown). Compared to Cas9 RNP, Cas9 in the form of mRNA resulted in a lower indel frequency. Thus, there seems to be a direct relationship between indel frequency and the DDR response. Further qPCR analysis indicated that the DDR is only apparent when a genome-targeting sgRNA is complexed with Cas9, suggesting that it is the active formation of a DSB that initiates the transcriptional DDR signature (Figure S10).

In terms of the ultimate effects of the editing process on cell survival, we observed both repression of cell cycle and induction of apoptosis within our treatments. The dramatic downregulation of cell cycle-related GO processes was observed only in Cas9 mRNA-treated samples, which appears to have occurred concurrently with the global metabolic and transcriptional repression unique to these samples. Although the same cell cycle inhibition did not appear in the other treatments (those exposed to electroporation, AAV6, and Cas9 RNP), we instead detected an upregulation of apoptotic processes. This effect could be due to the combined or individual effect of DNA damage, stress, and/or immune responses that were also observed in these treatment groups.

Transcriptional Response to Editing Machinery at Gene-Level Resolution

We next sought to identify the specific genes most heavily contributing to the various responses that we observed. In doing so, we identified all genes contributing to enrichment of GO processes for each category from Figure 3. For each of these categories, we then plotted the 10 genes that displayed the most highly significant fold change (median MLogP) across all donors for all treatments compared to appropriate control sample (Figure 4).

One of the most striking results was the dramatic upregulation of interferon-related genes when Cas9 mRNA was delivered to cells. In Cas9 mRNA-treated samples, we observed significant upregulation of the interferon regulatory factor gene family (*IRF1*, *IRF7*, and *IRF9*) *DDX58* (also known as RIG-I) that is known to induce the interferon response,[36] as well as interferons themselves (*IFI6*, *IFI16*, *IFNB1*) (Table S1). This is not surprising, since exogenous mRNAs have been shown to cause an interferon response in $CD34^+$ HSPCs,[37] with particular upregulation of *DDX58* and *IRF7*. Consistent with these findings, we also observed significant downstream effects of this response within genes that are reported to be induced by interferons, such as the 2′-5′-oligoadenylate synthetase gene family

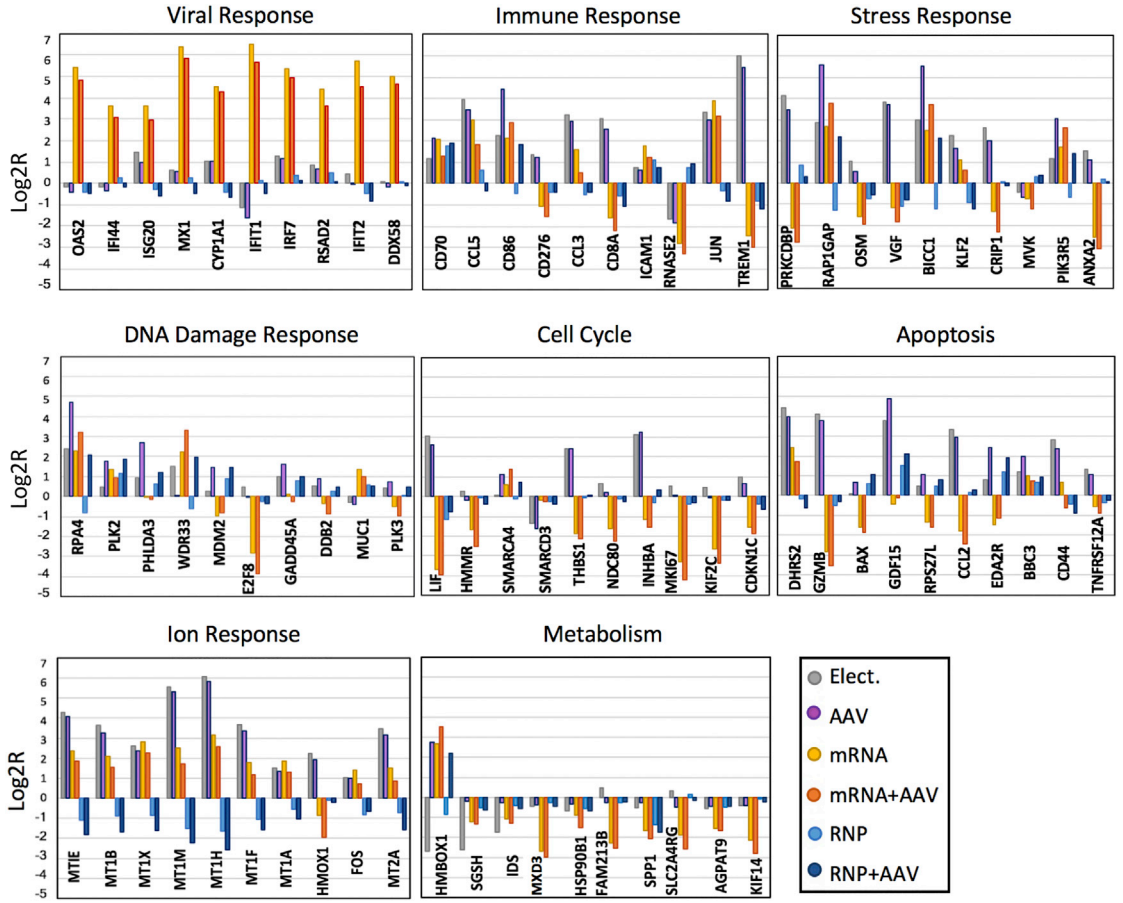

Figure 4. Gene-Level Resolution of the Most Heavily Enriched GO Processes

At 24 hr post-treatment, the genes contributing to GO enrichment were compiled and the top 10 most significantly differentially expressed genes in each GO category are shown (based on median MLogP values per GO category across all treatments). All differentially expressed genes as well as enriched GO processes are provided in Tables S1 and S2, respectively.

(*OAS1*, *OAS2*, *OAS3*, and *OASL*),[38] the interferon-inducible gene family (*IFI44L*, *IFIH1*, *IFIT1*, *IFIT2*, *IFIT5*, *IFITM1*, and *IFITM3*), as well as other interferon-inducible genes such as *MX1* and *RSAD2*, all of which displayed significant upregulation when cells were exposed to Cas9 mRNA.

Not only was the interferon response unique to Cas9 mRNA treatments, but we also observed dramatic transcriptional repression, particularly of cell cycle-related GOs. Along these lines, we observed significant downregulation of cell cycle regulator *HMMR* (also, known as RHAMM). We also observed significant downregulation of 13 cyclins (*CCNA1*, *CCNA2*, *CCNB1*, *CCNB2*, *CCND2*, *CCND3*, *CCNE1*, *CCNE2*, *CCNG1*, *CCNI*, *CCNK*, *CCNL2*, and *CCNY*), 13 cell-division cycle genes (*CDC7*, *CDC16*, *CDC20*, *CDC23*, *CDC25B*, *CDC25C*, *CDC26*, *CDC27*, *CDC34*, *CDC37*, *CDC42*, *CDC45*, and *CDC123*), 10 cyclin-dependent kinases (*CDK1*, *CDK2*, *CDK3*, *CDK4*, *CDK5*, *CDK6*, *CDK9*, *CDK10*, *CDK13*, and *CDK19*), and five cyclin-dependent kinase inhibitors (*CDKN1B*, *CDKN1C*, *CDKN2C*, *CDKN2D*, and *CDKN3*).

Though Cas9 mRNA drove the most dramatic transcriptional response, we observed upregulation of immune genes more uniformly across treatments. For instance, *JUN*, which plays a prominent role in innate and adaptive immunity, was upregulated across all treatment groups aside from those exposed to Cas9 RNP. We also observed common upregulation of apoptotic genes, such as *BBC3* (also known as PUMA), which is known to be upregulated in response to apoptotic stimuli.[39]

Apoptotic Inhibition during Genome Editing

Not only do components of the genome-editing machinery display differential effects on cell cycle and apoptotic regulation, but these may explain previously reported differences in cell viability and/or survival following the editing process (Extended Data Figures 1B and 5B from Dever et al.[8]). In order to replicate these findings, we performed an identical experiment and also found that delivery of Cas9 in the form of mRNA decreased viability as well as colony-forming ability by approximately 15% compared to Cas9 in the form of RNP (Figures S11A and S11B). These results demonstrate

not only that Cas9 mRNA elicits the greatest transcriptional response—characterized by a unique pattern of global transcriptional repression and cell cycle downregulation—but that it also causes the most dramatic effect on cell survival. Because of this loss of viability, even when incorporating well-tolerated chemical modifications into the mRNA and sgRNA, we began to consider whether inhibition of these responses would increase the viability of cells undergoing editing.

The pathway for apoptotic inhibition appears to be both less complicated and better understood than the complex processes of immune and stress responses. In addition, many small molecules have been reported to successfully inhibit apoptosis during cellular stress.[40] Therefore, we chose to focus our efforts on reducing the apoptotic response during the editing process. Toward this end, we first screened the effect of the following small-molecule apoptotic inhibitors on cell survival in K562 cells when administered following mock electroporation: BX795,[41] GSK2606414,[42] salubrinal,[43] and Z-VAD-FMK.[44] Across a wide range of concentrations, Z-VAD-FMK (1–100 μM) appeared to have the least potential for toxicity and displayed the greatest positive effect on cell viability and cell count as assessed by trypan blue staining at 96 hr post-electroporation (data not shown). We then tested the effect of Z-VAD-FMK addition (1–100 μM) during electroporation of Cas9 mRNA or RNP plus sgRNA in $CD34^+$ HSPCs. Using a more thorough analysis—assessing viability with Annexin V and PI, rather than trypan blue staining—we found no significant improvement in cell viability. However, this could be due to the high viability that we observed throughout the editing process, leaving little room for improvement (Figure S11A). In order to determine whether the addition of Z-VAD-FMK at time of editing could improve long-term survivability, we also performed a colony-forming assay using single-cell sorting into methylcellulose. This indicated that addition of Z-VAD-FMK (3–30 μM) could improve colony-forming ability, though this improvement did not achieve statistical significance (Figure S11B).

To further investigate the effect of apoptotic inhibition, we identified the upregulated genes from the microarrays that most heavily contributed to the apoptotic signature that we observed during RNP + AAV treatment. We then used this information to establish a qPCR assay that could rapidly gauge the level of apoptotic response to a given treatment. This allowed us to probe expression of a diverse set of genes acting in immune and DNA-damage-response pathways that have been linked to apoptosis, including *BAX*, *CD70*, *MDM2*, *RPS27L*, and *WDR33*. We performed this assay on the samples from Figure S11B in order not only to confirm that this apoptotic response was invoked by the editing process, but also to determine whether the addition of Z-VAD-FMK would be able to reduce this response at the transcriptional level. In doing so, we observed that the expression of all five genes was reduced when 10 μM of Z-VAD-FMK was added to the electroporation mixture in the full editing protocol (electroporation of RNP followed by AAV6 transduction) (Figure S11C). There also appeared to be a dose response, as the apoptotic signature returned as higher concentrations of Z-VAD-FMK were administered.

DISCUSSION

Artificial manipulation of cells and their environment often have negative effects on cell viability and survival. Cytotoxicity has been previously reported during genome editing in $CD34^+$ HSPCs depending on the type of manipulation.[8,45] However, prior to this study, it was unclear which components of the editing process and which underlying genes and pathways were most responsible for this deleterious response. By measuring genome-wide expression profiles, we identified transcriptional responses that were unique to various components of the editing protocol. And perhaps as expected, we also found that some pathways—particularly immune, stress, and apoptotic processes—were upregulated to varying degrees by all editing machinery components.

Of all components of the editing machinery, Cas9 mRNA elicited the most dramatic transcriptional effect (Figures 3, S8, S9, and S12). Compared to all other treatments, which had a relatively even split between up- and downregulated genes (Figure 2), the vast majority of differentially expressed probes in Cas9 mRNA-treated samples were downregulated. Among these probes, we found a particular enrichment of genes involved in metabolism and cell cycle regulation (Figures 3, S8, and S9). There was also an abundance of other seemingly unrelated processes that were coordinately downregulated (Figure S9B), suggestive of global transcriptional repression. These patterns occurred regardless of whether or not Cas9 mRNA delivery was followed by AAV6 transduction. Among the relatively few upregulated genes within Cas9 mRNA treatments, we observed the greatest enrichment of viral GO processes compared to all other treatments. This enrichment for viral processes, as well as the apparent global transcriptional repression, could be accounted for by the induction of the interferon response that was unique to Cas9 mRNA-treated samples. Toward this end, the interferon response has been previously observed when exogenous RNA is delivered to cells,[37] and this response has been shown to reduce global translation, likely in an effort to reduce production of viral proteins.[46,47] Our data suggests that this repressive response may be primarily mediated at the transcriptional level following exposure to non-specific, exogenous RNA, which is mistaken by the cell to be a virus (Figure S13). This reduction in global transcription (and likely translation) could account for the reduced rates of indel formation when Cas9 was delivered in the form of mRNA compared to protein pre-complexed with gRNA (Figures 1A and S12). For this reason, various modifications to the mRNA polymer have been tested and proven to minimize the innate immune response. We incorporated two of these, synthesizing the mRNA using 5-methylcytidine and pseudouridine, which have both been shown to dramatically reduce the interferon response relative to unmodified mRNAs.[20] Though these modified mRNAs are expected to be an improvement over their unmodified counterparts, which show reduced stability and translation, Cas9 in the form of RNP is much better tolerated by the cell in comparison. This, combined with the fact that Cas9 protein

complexed with sgRNA typically achieves higher indel rates and HR efficiency (Figure 1A),[8] demonstrates that Cas9 RNP is a safer and more effective alternative compared to Cas9 mRNA when delivered *ex vivo* by electroporation.

Likely as a result of the increased activity of Cas9 RNP, we observed the clearest DDR in this treatment (Figures 3, S8, and S14A). Cas9 is well-known to elicit a DDR, which is primarily thought to be a byproduct of off-target activity.[19] However, the sgRNA that we used has been shown to have limited off-target activity, with low levels of cutting observed at a single region outside the intended *HBB* locus.[8] This indicates that a single active cut site in the genome, one at which the majority of cutting and repair has occurred within the first 2 hr,[28] is enough to trigger a DDR that is detectable at the transcriptional level 24 hr later. This could be due to recurrent cutting that occurs at the cut site or simply a lag time involved in the transcriptional reaction to DNA damage. Because one of the best-established downstream effects of elevated DNA damage signaling is programmed cell death,[48] it is not surprising that Cas9 RNP-treated cells also showed an enrichment for apoptotic processes. However, the degree of additional apoptosis when Cas9 RNP is included in the electroporation solution (electroporation of Cas9 RNP compared to mock electroporation control) was consistently less than the apoptotic effect that results from mock electroporation and AAV transduction alone (as determined by comparison to non-electroporated controls). This indicates that electroporation and AAV transduction each contribute more heavily to the apoptosis observed following the full editing protocol than does the introduction of Cas9 RNP.

Prior to this study, we had hypothesized that a DDR could be initiated by AAV-mediated introduction of a single-stranded DNA (ssDNA) repair template. However, we found no detectable DDR at the transcriptional level in cells treated with AAV alone (Figure 3A). We had also expected AAV transduction to elicit an immune response, since systemic, humoral immune responses have been reported with recombinant AAV.[49,50] This has been shown to occur even though these recombinant vectors, in which all viral genes have been removed, display low immunogenicity compared to WT.[49] Nevertheless, we found that the most heavily enriched processes were in immune pathways (Figures 3, S8, and S14B). However, none of these immune processes were associated with viral or interferon responses. This was perhaps the greatest surprise—even though we identified a dramatic viral response with Cas9 mRNA treatment, exposure to bona fide virus in the form of recombinant AAV6 elicited no detectable viral response.

It should be noted that the results reported in this study were derived from a genome-editing protocol that yielded relatively low rates of HR (Figure 1A). However, these low rates do not appear to be due to inefficient delivery of genome-editing reagents (Figure S15). Rather, it has been reported that the HR rates can be dramatically boosted by simply altering the cell culture density of $CD34^+$ HSPCs in order to promote cell cycling, which is thought to be necessary for efficient HR.[51] Therefore, it would be of great interest to perform additional transcriptional analysis on HSPCs that have been targeted using the HR-optimized protocol.

To our knowledge, this is the first time that the transcriptional reaction to components of genome-editing machinery has been reported in non-immune primary cells. Our model system, editing of the SCD-associated locus in patient-derived HSPCs, is currently being taken to clinical trials. Gaining an understanding of the cellular response to the editing process, at the resolution of particular genes and pathways, allowed us to establish the comparative tolerance of the editing machinery and to indicate how this process could be refined. Although it may not be possible to eliminate all of the negative effects of the editing process, electroporation of Cas9 in the form of RNP followed by AAV6-mediated delivery of the template for HR represents an extraordinarily well-tolerated approach. This is in comparison to Cas9 delivered as a chemically modified mRNA, which is known to be much better tolerated than unmodified mRNA as well as DNA plasmid-based delivery. These data now provide a baseline by which to evaluate the transcriptional response of cells targeted with mRNA or sgRNA with alternative chemical modifications. Moreover, given the broad use of ssODNs in genome editing, it would be of interest to perform a similar analysis of the transcriptional response to ssODN-mediated targeting in clinically relevant human cells.

In summary, these data establish a benchmark for cellular tolerance of the most modern genome-editing process and to which further refinements may be compared. In doing so, we will ensure that genome editing is as safe and efficient as it can possibly be and therefore maximize its translation to the clinic.

MATERIALS AND METHODS

AAV Production and Purification

The Glu6Val (E6V) AAV6 plasmid was cloned into pAAV-MCS plasmid (Agilent Technologies) containing AAV2 inverted terminal repeats (ITRs). The single-stranded donor contained 2.2 kb of homologous sequence both upstream and downstream of Glu6Val.[8] AAV was produced as described previously.[52] Each 15-cm^2 dish of 293FT cells (Life Technologies) was transfected using polyethylenimine (PEI) (linear, MW 25K) along with 6 μg ITR-containing plasmid and 22 μg pDGM6 (gift from D. Russell), which contains AAV6 cap, AAV2 rep, and adenoviral helper genes. 72 hr post-transfection, cells were harvested and lysed by freeze-thaw cycles and purified using an iodixanol density gradient by ultracentrifugation. AAV6 vectors were then extracted from the 40%–60% iodixanol interface and exchanged into PBS with 5% sorbitol using an Amicon centrifugal filter 100K MWCO (Millipore Sigma) following the manufacturer's instructions. Vectors were titered after buffer exchange using qPCR as described previously.[30]

Cell Culture

$CD34^+$ HSPCs used for gene expression microarrays were obtained as frozen stock derived from mobilized peripheral blood thawed according to manufacturer's instructions (AllCells). For follow-up experiments, $CD34^+$ HSPCs were obtained fresh from cord blood from

donors under informed consent via the Binns Program for Cord Blood Research at Stanford University. $CD34^+$ HSPCs were purified using the CD34 MicroBead Kit UltraPure (Miltenyi Biotec) according to manufacturer's protocol. In brief, cells were cultured overnight then stained using APC anti-human CD34 (BioLegend) and BD Horizon V450 anti-human CD45 (BD Biosciences). HSPCs were then obtained by sorting the $CD34^{bright}/CD45^{dim}$ population on a FACS Aria II cell sorter (BD Biosciences). HSPCs were cultured in StemSpan SFEM II (StemCell Technologies) supplemented with UM171 (35 nM), TPO (100 ng/mL), SCF (100 ng/mL), Flit 3 ligand (100 ng/mL), interleukin-6 (IL-6) (100 ng/mL), Stem Regenin 1 (0.75 mM), 20 mg/mL streptomycin, and 20 U/mL penicillin. K562 cells were cultured in RPMI 1640 (HyClone) supplemented with 10% bovine growth serum, 100 mg/mL streptomycin, 100 U/mL penicillin, and 2 mM L-glutamine. All cells were cultured at 37°C with 5% CO_2. K562 cells were cultured at ambient O_2 and $CD34^+$ HSPCs were cultured at 5% O_2. Cells were cultured at densities ranging from 1E5-1E6 cells/mL.

$CD34^+$ HSPC Electroporation and Transduction

The R-02 sgRNA used to target the *HBB* locus was synthesized with chemically modified nucleotides containing 2′-O-methyl-3′-phosphorothioate at the three terminal positions at both 5′ and 3′ ends (HPLC purified; Agilent Technologies). The genomic sgRNA target sequence is 5′-C TTGCCCCACAGGGCAGTAA**CGG**-3′ (PAM in bold).[53,54] Cas9 mRNA was synthesized with 5-methylcytidine and pseudouridine (TriLink BioTechnologies). To form RNP, Cas9 protein (Life Technologies) was complexed with sgRNA at a molar ratio of 2:5 at 25°C for 10 min immediately prior to electroporation. $CD34^+$ HSPCs were electroporated 1–2 days after thawing. For each treatment analyzed with gene expression microarrays, 1E6 cells were resuspended in buffer 1 M[55] and electroporated using the Lonza Nucleofector 2b (program U-014). For follow-up experiments, $CD34^+$ HSPCs were electroporated using the Lonza 4D-Nucleofector (program DZ-100). As appropriate, the following conditions were used: 150 μg/mL Cas9 mRNA with 100 μg/mL sgRNA, 300 μg/mL Cas9 protein complexed with sgRNA. Following electroporation, appropriate treatments were transduced with AAV6 at an MOI of 5E4 and incubated at 37°C until harvest at 6-hr, 24-hr, and 7-day time points.

Measuring Indel and HR Frequencies

$CD34^+$ HSPCs were harvested 7 days post-electroporation to determine indel and HR frequencies. Genomic DNA was harvested with QuickExtract (Epicenter) and was used for PCR of the *HBB* cut site with the following primers: forward, 5′-CCAACTCCTAAGCCAGT GCCAGAAGAG-3′; reverse, 5′-AGTCAGTGCCTATCAGAAACC CAAGAG-3′. TIDER software was used to estimate indel frequency using Sanger sequences of the PCR amplicons.[32] In order to assess HR frequencies, the following primers were used to amplify the targeted region: forward (outside homology arm), 5′-GGTGACAAT TTCTGCCAATCAGG-3′; reverse (inside homology arm), 5′-GAA TGGTAGCTGGATTGTAGCTGC-3′. The amplicon was gel purified and re-amplified using nested PCR with the following primers: forward, 5′-GAAGATATGCTTAGAACCGAGG−3′; reverse, 5′-CCA CATGCCCAGTTTCTATTGG-3′. This amplicon was gel-purified and cloned into a TOPO plasmid using the Zero Blunt TOPO PCR Cloning Kit (Life Technologies) according to manufacturer's instructions. TOPO reactions were transformed into competent *E. coli* and plated on kanamycin-containing agar plates. 100 single colonies were subjected to rolling circle amplification by MCLab and sequenced using the following primer: 5′-GAAGATATGCTT AGAACCGAGG-3′.

Microarray-Based Gene Expression Measurements

Two-fifths of the total number of cells were harvested from each treatment for each of four donors at both 6 hr and 24 hr (with exception of non-electroporated controls and AAV-only samples, which were collected only at 24 hr) and subjected to RNA extraction. Fluorescently Cy3-labeled cRNA was generated from 100 nanograms of total RNA for each sample per time point using the Agilent One-Color Low Input Quick Amp Labeling Kit (5190-2305). Labeled cRNA was fragmented and hybridized in duplicate to gene-expression microarrays (Agilent SurePrint G3 Human Gene Expression v3 8x60K Microarray, G4858A-072363) for 17 hr at 65°C. After washing, all microarrays were scanned in a single run in random order at default settings for an Agilent C Scanner using a single pass over the scan area at a resolution of 3 μm and a 20-bit scan type. Data was extracted with Agilent Feature Extraction Software (version 12.0.5.3) using the default settings for the one-color protocol. All processed green signals from transcripts measured on the array were used as input for unsupervised clustering by PCA as implemented by the FactoMineR package in R (http://www.r-project.org). For each scanned feature per treatment, median log2 ratio of expression levels was calculated as log2(treatment/appropriate control). This value was then averaged across all donors and replicates. Using a two-way ANOVA, we determined the likelihood that the observed fold change among the four donors for each scanned feature is entirely due to chance (displayed as −log10(p value) or "MLogP"). MLogP values greater than 7 should be considered highly significant after Bonferroni correction.

GO Enrichment Analysis

To evaluate enrichment of particular GOs within upregulated or downregulated gene sets, all genes that met the Bonferonni-corrected significance threshold (MLogP $\geq$ 7) were determined for each treatment group at each time point. Those with positive log2R values were included in the upregulated target gene set and those with negative values in the downregulated target gene set. These were then used as input as unranked lists of target genes against the unranked background set of all genes on the array into the GOrilla GO enrichment analysis tool (http://cbl-gorilla.cs.technion.ac.il/).[33] GOrilla reports the FDR q value of each GO term following Benjamini-Hochberg correction for multiple testing, and those GO processes with FDR $\leq$ 0.01 were considered to be highly significant.

Apoptotic Inhibitor Screen

For the initial screen, 1E6 K562 cells were resuspended in nucleofection buffer containing 100 mM KH_2PO_4, 15 mM $NaHCO_3$, 12 mM

$MgCl_2 \times 6H_2O$, 8 mM ATP, 2 mM glucose and then electroporated using the Lonza 2b Nucleofector (program T-016). 5E4 cells were placed into individual wells of a 48-well plate at a density of 1E5 cells/mL and treatments of one of the following were added to each well: BX795 (final concentration of 10 nM–20 μM) (Fisher Scientific), GSK2606414 (3 nM–10 μM) (Fisher Scientific), salubrinal (100 nM–75 μM) (Santa Cruz Biotechnology), and Z-VAD-FMK (1–100 μM) (Fisher Scientific). 4 days post-electroporation, cells were analyzed for viability using trypan blue stain using an automated cell counter. After the initial findings in K562 cells, $CD34^+$ HSPCs were isolated, cultured, and targeted as above, and Z-VAD-FMK was added to the electroporation mixture following electroporation (at a final post-dilution concentration of 1–100 μM) and viability was analyzed 24 hr post-electroporation using Annexin V/PI staining.

qPCR Assay

We designed a qPCR panel in which we probed expression of apoptosis-linked genes in order to rapidly gauge the apoptotic responses to various treatments. RNA was extracted from cells and converted to cRNA using SuperScript III First-Strand Synthesis (Invitrogen). qPCR was then performed on a LightCycler480 machine (Roche) using Fast EvaGreen qPCR Master Mix (Biotium) according to manufacturer's instructions. Cycling times were as follows: (1) 98°C, 2 min initial denaturation; (2) 98°C, 5 s denaturation; (3) 60°C 20 s annealing and extension; (4) return to step 2 39×. Relative expression levels of individual genes were determined within each sample by comparison to *RPLP0* control probe (assay ID, Hs99999902_m1; Applied Biosystems).

Methylcellulose Colony-Formation Assay

The colony-forming unit (CFU) assay was performed by FACS single-cell sorting of live (Annexin V^-/PI^-) $CD34^+$ cells into 96-well plates containing MethoCult Optimum (StemCell Technologies) 2 days post-electroporation. At 15 days post-sorting, total numbers of colonies were counted and compared to the total number of cells sorted to yield percentage colony formation.

SUPPLEMENTAL INFORMATION

Supplemental Information includes fifteen figures, two tables, and two data files and can be found with this article online at https://doi.org/10.1016/j.ymthe.2018.06.002.

AUTHOR CONTRIBUTIONS

M.K.C., S.V., and A.H. performed genome editing and follow-up analysis. M.K.C., S.R.H., and R.M.M. performed and analyzed qPCR assays. M.K.C. and M.K. performed and analyzed apoptotic inhibition experiments. M.K.C. and J.C. performed and analyzed methylcellulose assays. D.E.R., A.B.L., and L.B. performed biochemistry for microarrays. M.K.C., B.C., and I.S. performed bioinformatics analysis. R.O.B. and D.P.D. contributed to experimental design and data interpretation. A.H. and M.H.P. directed the research and participated in the design and interpretation of the experiments. M.K.C. wrote the manuscript with help from all authors.

CONFLICTS OF INTEREST

M.H.P. is a member of the scientific advisory board of CRISPR Therapeutics and holds equity in CRISPR Therapeutics, but the company had no input into any aspect of this work. D.E.R., B.C., A.B.L., I.S., and L.B. are employees of Agilent Technologies.

ACKNOWLEDGMENTS

We would like to thank D. Russell for the pDGM6 plasmid and the Binns Program for Cord Blood Research at Stanford University for cord blood-derived $CD34^+$ HSPCs. We also would like to give thanks to the members of the Porteus laboratory for input, comments, and discussion. M.H.P. gratefully acknowledges the support of the Amon Carter Foundation, the Laurie Kraus Lacob Faculty Scholar Award in Pediatric Translational Research, the Sutardja Foundation, and NIH grant support (R01-AI097320 and R01-AI120766). M.K.C. was supported by an NIH T32 Institutional Training Grant in Hematology (5T32HL120824-04). D.P.D. was supported by the Stanford Child Health Research Institute (CHRI) grant and the Bass Cancer Center Program Endowment. R.O.B. was supported through an Individual Postdoctoral grant (DFF-1333-00106B) and a Sapere Aude Research Talent grant (DFF-1331-00735B), both from the Danish Council for Independent Research, Medical Sciences.

REFERENCES

1. Takata, M., Sasaki, M.S., Sonoda, E., Morrison, C., Hashimoto, M., Utsumi, H., Yamaguchi-Iwai, Y., Shinohara, A., and Takeda, S. (1998). Homologous recombination and non-homologous end-joining pathways of DNA double-strand break repair have overlapping roles in the maintenance of chromosomal integrity in vertebrate cells. EMBO J. *17*, 5497–5508.

2. Hsu, P.D., Lander, E.S., and Zhang, F. (2014). Development and applications of CRISPR-Cas9 for genome engineering. Cell *157*, 1262–1278.

3. Doudna, J.A., and Charpentier, E. (2014). Genome editing. The new frontier of genome engineering with CRISPR-Cas9. Science *346*, 1258096.

4. Jinek, M., Chylinski, K., Fonfara, I., Hauer, M., Doudna, J.A., and Charpentier, E. (2012). A programmable dual-RNA-guided DNA endonuclease in adaptive bacterial immunity. Science *337*, 816–821.

5. Cong, L., Ran, F.A., Cox, D., Lin, S., Barretto, R., Habib, N., Hsu, P.D., Wu, X., Jiang, W., Marraffini, L.A., and Zhang, F. (2013). Multiplex genome engineering using CRISPR/Cas systems. Science *339*, 819–823.

6. Neumann, E., Schaefer-Ridder, M., Wang, Y., and Hofschneider, P.H. (1982). Gene transfer into mouse lyoma cells by electroporation in high electric fields. EMBO J. *1*, 841–845.

7. Hendel, A., Bak, R.O., Clark, J.T., Kennedy, A.B., Ryan, D.E., Roy, S., Steinfeld, I., Lunstad, B.D., Kaiser, R.J., Wilkens, A.B., et al. (2015). Chemically modified guide RNAs enhance CRISPR-Cas genome editing in human primary cells. Nat. Biotechnol. *33*, 985–989.

8. Dever, D.P., Bak, R.O., Reinisch, A., Camarena, J., Washington, G., Nicolas, C.E., Pavel-Dinu, M., Saxena, N., Wilkens, A.B., Mantri, S., et al. (2016). CRISPR/Cas9 β-globin gene targeting in human haematopoietic stem cells. Nature *539*, 384–389.

9. Lombardo, A., Genovese, P., Beausejour, C.M., Colleoni, S., Lee, Y.L., Kim, K.A., Ando, D., Urnov, F.D., Galli, C., Gregory, P.D., et al. (2007). Gene editing in human stem cells using zinc finger nucleases and integrase-defective lentiviral vector delivery. Nat. Biotechnol. *25*, 1298–1306.

10. Chen, F., Pruett-Miller, S.M., Huang, Y., Gjoka, M., Duda, K., Taunton, J., Collingwood, T.N., Frodin, M., and Davis, G.D. (2011). High-frequency genome editing using ssDNA oligonucleotides with zinc-finger nucleases. Nat. Methods *8*, 753–755.

11. Porteus, M.H., Cathomen, T., Weitzman, M.D., and Baltimore, D. (2003). Efficient gene targeting mediated by adeno-associated virus and DNA double-strand breaks. Mol. Cell. Biol. *23*, 3558–3565.

12. Miller, D.G., Petek, L.M., and Russell, D.W. (2003). Human gene targeting by adeno-associated virus vectors is enhanced by DNA double-strand breaks. Mol. Cell. Biol. *23*, 3550–3557.

13. Kaulich, M., and Dowdy, S.F. (2015). Combining CRISPR/Cas9 and rAAV Templates for Efficient Gene Editing. Nucleic Acid Ther. *25*, 287–296.

14. Sather, B.D., Romano Ibarra, G.S., Sommer, K., Curinga, G., Hale, M., Khan, I.F., Singh, S., Song, Y., Gwiazda, K., Sahni, J., et al. (2015). Efficient modification of CCR5 in primary human hematopoietic cells using a megaTAL nuclease and AAV donor template. Sci. Transl. Med. *7*, 307ra156.

15. Wang, J., Exline, C.M., DeClercq, J.J., Llewellyn, G.N., Hayward, S.B., Li, P.W.L., Shivak, D.A., Surosky, R.T., Gregory, P.D., Holmes, M.C., and Cannon, P.M. (2015). Homology-driven genome editing in hematopoietic stem and progenitor cells using ZFN mRNA and AAV6 donors. Nat. Biotechnol. *33*, 1256–1263.

16. De Ravin, S.S., Reik, A., Liu, P.Q., Li, L., Wu, X., Su, L., Raley, C., Theobald, N., Choi, U., Song, A.H., et al. (2016). Targeted gene addition in human CD34(+) hematopoietic cells for correction of X-linked chronic granulomatous disease. Nat. Biotechnol. *34*, 424–429.

17. Morgens, D.W., Wainberg, M., Boyle, E.A., Ursu, O., Araya, C.L., Tsui, C.K., Haney, M.S., Hess, G.T., Han, K., Jeng, E.E., et al. (2017). Genome-scale measurement of off-target activity using Cas9 toxicity in high-throughput screens. Nat. Commun. *8*, 15178.

18. Chew, W.L., Tabebordbar, M., Cheng, J.K., Mali, P., Wu, E.Y., Ng, A.H., Zhu, K., Wagers, A.J., and Church, G.M. (2016). A multifunctional AAV-CRISPR-Cas9 and its host response. Nat. Methods *13*, 868–874.

19. Aguirre, A.J., Meyers, R.M., Weir, B.A., Vazquez, F., Zhang, C.Z., Ben-David, U., Cook, A., Ha, G., Harrington, W.F., Doshi, M.B., et al. (2016). Genomic Copy Number Dictates a Gene-Independent Cell Response to CRISPR/Cas9 Targeting. Cancer Discov. *6*, 914–929.

20. Warren, L., Manos, P.D., Ahfeldt, T., Loh, Y.H., Li, H., Lau, F., Ebina, W., Mandal, P.K., Smith, Z.D., Meissner, A., et al. (2010). Highly efficient reprogramming to pluripotency and directed differentiation of human cells with synthetic modified mRNA. Cell Stem Cell *7*, 618–630.

21. Lee, K., Mackley, V.A., Rao, A., Chong, A.T., Dewitt, M.A., Corn, J.E., and Murthy, N. (2017). Synthetically modified guide RNA and donor DNA are a versatile platform for CRISPR-Cas9 engineering. eLife *6*, e25312.

22. Rahdar, M., McMahon, M.A., Prakash, T.P., Swayze, E.E., Bennett, C.F., and Cleveland, D.W. (2015). Synthetic CRISPR RNA-Cas9-guided genome editing in human cells. Proc. Natl. Acad. Sci. USA *112*, E7110–E7117.

23. Cvetković, D.M., Živanović, M.N., Milutinović, M.G., Djukić, T.R., Radović, M.D., Cvetković, A.M., Filipović, N.D., and Zdravković, N.D. (2016). Real-time monitoring of cytotoxic effects of electroporation on breast and colon cancer cell lines. Bioelectrochemistry. , Published online October 22, 2016. https://doi.org/10.1016/j.bioelechem.2016.10.005.

24. Howard, D.B., Powers, K., Wang, Y., and Harvey, B.K. (2008). Tropism and toxicity of adeno-associated viral vector serotypes 1, 2, 5, 6, 7, 8, and 9 in rat neurons and glia in vitro. Virology *372*, 24–34.

25. Hoban, M.D., Orkin, S.H., and Bauer, D.E. (2016). Genetic treatment of a molecular disorder: gene therapy approaches to sickle cell disease. Blood *127*, 839–848.

26. Stamatoyannopoulos, G. (1972). The molecular basis of hemoglobin disease. Annu. Rev. Genet. *6*, 47–70.

27. Ling, C., Bhukhai, K., Yin, Z., Tan, M., Yoder, M.C., Leboulch, P., Payen, E., and Srivastava, A. (2016). High-Efficiency Transduction of Primary Human Hematopoietic Stem/Progenitor Cells by AAV6 Vectors: Strategies for Overcoming Donor-Variation and Implications in Genome Editing. Sci. Rep. *6*, 35495.

28. Rose, J.C., Stephany, J.J., Valente, W.J., Trevillian, B.M., Dang, H.V., Bielas, J.H., Maly, D.J., and Fowler, D.M. (2017). Rapidly inducible Cas9 and DSB-ddPCR to probe editing kinetics. Nat. Methods *14*, 891–896.

29. Zolotukhin, S., Byrne, B.J., Mason, E., Zolotukhin, I., Potter, M., Chesnut, K., Summerford, C., Samulski, R.J., and Muzyczka, N. (1999). Recombinant adeno-associated virus purification using novel methods improves infectious titer and yield. Gene Ther. *6*, 973–985.

30. Aurnhammer, C., Haase, M., Muether, N., Hausl, M., Rauschhuber, C., Huber, I., Nitschko, H., Busch, U., Sing, A., Ehrhardt, A., and Baiker, A. (2012). Universal real-time PCR for the detection and quantification of adeno-associated virus serotype 2-derived inverted terminal repeat sequences. Hum. Gene Ther. Methods *23*, 18–28.

31. Brinkman, E.K., Chen, T., Amendola, M., and van Steensel, B. (2014). Easy quantitative assessment of genome editing by sequence trace decomposition. Nucleic Acids Res. *42*, e168.

32. Brinkman, E.K., Kousholt, A.N., Harmsen, T., Leemans, C., Chen, T., Jonkers, J., and van Steensel, B. (2018). Easy quantification of template-directed CRISPR/Cas9 editing. Nucleic Acids Res. *46*, e58.

33. Eden, E., Navon, R., Steinfeld, I., Lipson, D., and Yakhini, Z. (2009). GOrilla: a tool for discovery and visualization of enriched GO terms in ranked gene lists. BMC Bioinformatics *10*, 48.

34. Pinkham, C., Dahal, B., de la Fuente, C.L., Bracci, N., Beitzel, B., Lindquist, M., Garrison, A., Schmaljohn, C., Palacios, G., Narayanan, A., et al. (2017). Alterations in the host transcriptome in vitro following Rift Valley fever virus infection. Sci. Rep. *7*, 14385.

35. Ivashkiv, L.B., and Donlin, L.T. (2014). Regulation of type I interferon responses. Nat. Rev. Immunol. *14*, 36–49.

36. Loo, Y.M., and Gale, M., Jr. (2011). Immune signaling by RIG-I-like receptors. Immunity *34*, 680–692.

37. Schiroli, G., Ferrari, S., Conway, A., Jacob, A., Capo, V., Albano, L., Plati, T., Castiello, M.C., Sanvito, F., Gennery, A.R., et al. (2017). Preclinical modeling highlights the therapeutic potential of hematopoietic stem cell gene editing for correction of SCID-X1. Sci. Transl. Med. *9*, eaan0820.

38. Sadler, A.J., and Williams, B.R. (2008). Interferon-inducible antiviral effectors. Nat. Rev. Immunol. *8*, 559–568.

39. Han, J., Flemington, C., Houghton, A.B., Gu, Z., Zambetti, G.P., Lutz, R.J., Zhu, L., and Chittenden, T. (2001). Expression of bbc3, a pro-apoptotic BH3-only gene, is regulated by diverse cell death and survival signals. Proc. Natl. Acad. Sci. USA *98*, 11318–11323.

40. Derakhshan, A., Chen, Z., and Van Waes, C. (2017). Therapeutic Small Molecules Target Inhibitor of Apoptosis Proteins in Cancers with Deregulation of Extrinsic and Intrinsic Cell Death Pathways. Clin. Cancer Res. *23*, 1379–1387.

41. Clark, K., Plater, L., Peggie, M., and Cohen, P. (2009). Use of the pharmacological inhibitor BX795 to study the regulation and physiological roles of TBK1 and IkappaB kinase epsilon: a distinct upstream kinase mediates Ser-172 phosphorylation and activation. J. Biol. Chem. *284*, 14136–14146.

42. Weng, S., Zhou, L., Deng, Q., Wang, J., Yu, Y., Zhu, J., and Yuan, Y. (2016). Niclosamide induced cell apoptosis via upregulation of ATF3 and activation of PERK in Hepatocellular carcinoma cells. BMC Gastroenterol. *16*, 25.

43. Cnop, M., Ladriere, L., Hekerman, P., Ortis, F., Cardozo, A.K., Dogusan, Z., Flamez, D., Boyce, M., Yuan, J., and Eizirik, D.L. (2007). Selective inhibition of eukaryotic translation initiation factor 2 alpha dephosphorylation potentiates fatty acid-induced endoplasmic reticulum stress and causes pancreatic beta-cell dysfunction and apoptosis. J. Biol. Chem. *282*, 3989–3997.

44. Saini, U., Gumina, R.J., Wolfe, B., Kuppusamy, M.L., Kuppusamy, P., and Boudoulas, K.D. (2013). Preconditioning mesenchymal stem cells with caspase inhibition and hyperoxia prior to hypoxia exposure increases cell proliferation. J. Cell. Biochem. *114*, 2612–2623.

45. Genovese, P., Schiroli, G., Escobar, G., Tomaso, T.D., Firrito, C., Calabria, A., Moi, D., Mazzieri, R., Bonini, C., Holmes, M.C., et al. (2014). Targeted genome editing in human repopulating haematopoietic stem cells. Nature *510*, 235–240.

46. Kaur, S., Sassano, A., Dolniak, B., Joshi, S., Majchrzak-Kita, B., Baker, D.P., Hay, N., Fish, E.N., and Platanias, L.C. (2008). Role of the Akt pathway in mRNA translation of interferon-stimulated genes. Proc. Natl. Acad. Sci. USA *105*, 4808–4813.

47. Guo, J., Hui, D.J., Merrick, W.C., and Sen, G.C. (2000). A new pathway of translational regulation mediated by eukaryotic initiation factor 3. EMBO J. *19*, 6891–6899.

48. Norbury, C.J., and Zhivotovsky, B. (2004). DNA damage-induced apoptosis. Oncogene *23*, 2797–2808.

49. Sun, J.Y., Anand-Jawa, V., Chatterjee, S., and Wong, K.K. (2003). Immune responses to adeno-associated virus and its recombinant vectors. Gene Ther. *10*, 964–976.

50. Zaiss, A.K., Liu, Q., Bowen, G.P., Wong, N.C., Bartlett, J.S., and Muruve, D.A. (2002). Differential activation of innate immune responses by adenovirus and adeno-associated virus vectors. J. Virol. *76*, 4580–4590.

51. Charlesworth, C.T., Camarena, J., Cromer, M.K., Vaidyanathan, S., Bak, R.O., Carte, J., Potter, J., Dever, D.P., and Porteus, M.H. (2018). Priming human repopulating hematopoietic stem and progenitor cells for Cas9/sgRNA gene targeting. Mol. Ther. Nucleic Acids *12*, 89–104.

52. Khan, I.F., Hirata, R.K., and Russell, D.W. (2011). AAV-mediated gene targeting methods for human cells. Nat. Protoc. *6*, 482–501.

53. Hendel, A., Kildebeck, E.J., Fine, E.J., Clark, J., Punjya, N., Sebastiano, V., Bao, G., and Porteus, M.H. (2014). Quantifying genome-editing outcomes at endogenous loci with SMRT sequencing. Cell Rep. *7*, 293–305.

54. Cradick, T.J., Fine, E.J., Antico, C.J., and Bao, G. (2013). CRISPR/Cas9 systems targeting β-globin and CCR5 genes have substantial off-target activity. Nucleic Acids Res. *41*, 9584–9592.

55. Chicaybam, L., Sodre, A.L., Curzio, B.A., and Bonamino, M.H. (2013). An efficient low cost method for gene transfer to T lymphocytes. PLoS ONE *8*, e60298.